Journal of Hazardous Materials 196 (2011) 287–294

Contents lists available at SciVerse ScienceDirect

Journal of Hazardous Materials

journal homepage: www.elsevier.com/locate/jhazmat

Valorisation of electric arc furnace steel slag as raw material for low energy belite cements

R.I. Iacobescu[a], D. Koumpouri[b], Y. Pontikes[c], R. Saban[a], G.N. Angelopoulos[b,*]

[a] Department of Materials Science and Engineering, Politehnica University of Bucharest, Splaiul Independentei 313, 060032 Bucharest, Romania
[b] Laboratory of Materials and Metallurgy, Department of Chemical Engineering, University of Patras, 26500 Rio, Greece
[c] Department of Metallurgy and Materials Engineering, Katholieke Universiteit Leuven, Kasteelpark Arenberg 44 bus 2450, B-3001 Heverlee (Leuven), Belgium

ARTICLE INFO

Article history:
Received 5 July 2011
Received in revised form 7 September 2011
Accepted 7 September 2011
Available online 12 September 2011

Keywords:
Electric arc furnace slag
Belite cement

ABSTRACT

In this paper, the valorisation of electric arc furnace steel slag (EAFS) in the production of low energy belite cements is studied. Three types of clinkers were prepared with 0 wt.% (BC), 5 wt.% (BC5) and 10 wt.% (BC10) EAFS, respectively. The design of the raw mixes was based on the compositional indices lime saturation factor (LSF), alumina ratio (AR) and silica ratio (SR). The clinkering temperature was studied for the range 1280–1400 °C; firing was performed at 1380 °C based on the results regarding free lime and the evolution of microstructure. In order to activate the belite, clinkers were cooled fast by blown air and concurrent crushing. The results demonstrate that the microstructure of the produced clinkers is dominated by belite and alite crystals, with tricalcium aluminate and tetracalcium-alumino-ferrite present as micro-crystalline interstitial phases. The prepared cements presented low early strength development as expected for belite-rich compositions; however the 28-day results were 47.5 MPa, 46.6 MPa and 42.8 MPa for BC, BC5 and BC10, respectively. These values are comparable with OPC CEMI 32.5 N (32.5–52.5 MPa) according to EN 197-1. A fast setting behaviour was also observed, particularly in the case of BC10, whereas soundness did not exceed 1 mm.

1. Introduction

Recent years have seen the cement industry growing dynamically with most of the activity taking place in emerging economies. Despite financial turbulence, population growth and the resulting need for housing along with state investments in infrastructure are strong drivers to offset the downturn in cement markets. Globally, cement production increased from 2.568 Mt in 2006 to 3.294 Mt in 2010 [1].

Unavoidably, as with any industrial activity, cement production has its own environmental footprint. Estimations suggest that cement production is responsible for 5–7% of the worldwide CO_2 emission [2,3]. If all the greenhouse gases emitted by anthropogenic activities are considered, the cement manufacturing industry contributes about 3% of the total anthropogenic greenhouse gases emissions [2]. This is predominantly the result of the fuels used to generate the required energy, estimated at 0.37 kg/kg clinker, and of the de-carbonation of limestone ($CaCO_3$) which takes place during cement production, estimated at 0.53 kg/kg clinker CO_2 [2]. Consequently, reducing the limestone in the raw meal and thus changing its chemistry, could lead to lower CO_2 emissions. This potential has resulted in increased scientific interest in innovative types of cement [4], and more specifically, in belite-rich cements over the last 20 years [5,6]. This type of cement, unlike conventional OPC, contains a higher percentage of belite (C_2S) and a lower percentage of alite (C_3S). In order to reach the desirable percentages of C_2S and C_3S, the lime saturation factor (LSF) must be between 78% and 83% [7]. The environmental benefits of the belite type cements over OPC can be summarized as follows: energy saving could rise up to 16% [8], burning temperatures could be reduced by 6–10% and levels of emitted CO_2 and NO_x could fall [9,10]. However, the early strength of such cements is lower and milling energy might be increased due to the hardness of C_2S. By combining the production of belite cements with alternative raw materials as a substitute for limestone, such as metallurgical slag's, additional benefits may be obtained [11].

During the production of iron and steel, several types of slag are generated. These include blast furnace (BF), basic oxygen furnace (BOF), electric arc furnace (EAF) and stainless steel (SS-EAF and SS-AOD) slag. Nearly 50 Mt/y of steel slag is produced globally and 12 Mt/y is produced in Europe [12]. About 65% of this is used in qualified fields of applications, mainly construction, while the remainder is stored or used for other small purposes [13]. Around 37% of the steel slag produced in Europe in 2010 was used for cement production [14].

Nowadays more than 40% of global steel production takes place in EAFs [15] and is associated with 20 Mt/y slag generation. Greece has a cement production capacity of approximately 18 Mt/y [16],

* Corresponding author. Tel.: +30 2610969530; fax: +30 2610990917.
E-mail address: angel@chemeng.upatras.gr (G.N. Angelopoulos).

0304-3894/$ – see front matter © 2011 Elsevier B.V. All rights reserved.
doi:10.1016/j.jhazmat.2011.09.024

and a steel production capacity of 3.5 Mt/y. The annual EAF slag (EAFS) production varies from 300.000 t/y to 400.000 t/y. Of the total amount of EAFS processed annually, around 55% is used in the production of coarse aggregates for road construction. The main environmental problems associated with the disposal of the wasted EAFS are the "dusting" of the slag and the release of leachates. Thus, quite apart from the needs of the cement industries, steel producers have their own motivations for finding a use for their slag.

In principle, there are two methods of incorporating slag in cement production: either in the raw meal or in a later stage, as a (latent) hydraulic or pozzolanic material [17]. Prior studies indicate that an EAFS addition of up to 10 wt.% in the raw meal is effective without any detrimental effect on the technical properties of the resultant cement [17]. Other authors reached similar results, in terms of sintering, microstructure, as well as, hydrating properties of the final clinker with 10.5 wt.% EAFS addition. In addition to the above, other authors suggest that the addition of EAFS in clinker production will reduce the sintering temperature of raw meal and the theoretic heat consumption [18]. Moreover, cement containing steel slag as BOF and/or EAF can also have improved corrosion resistance than conventional Portland cement [19]. Finally, combinations of EAFS, BOF and AOD slags were tested for the production of sulfo-aluminate belite cements with encouraging results [20]. Despite the work in the field, no studies were focused on the use of EAFS for belite-rich cements to the best of our knowledge.

In terms of disadvantages, the heavy metals content (Cr, V, etc.) in steel slag is an issue of concern. In the European Union (EU), a directive regarding Cr(VI) came into effect in 2005 and prohibits the use or supply of cements containing more than 2 ppm water-soluble chromium by mass of cement [21]. Typically, Cr(VI) compounds are more water-soluble (although insoluble do exist as well), thus more likely to participate in leaching. A number of adverse health effects have been associated with Cr(VI) exposure, ranging in severity. According to NIOSH [22] all Cr(VI) compounds are considered potential occupational carcinogens. Reducing agents, such as ferrous sulphate, either the monohydrate ($FeSO_4{\cdot}H_2O$) or heptahydrate ($FeSO_4{\cdot}7H_2O$) form, or stannous sulphate ($SnSO_4$) are added to control the oxidation state of chromium [23].

The present work explores how EAFS can be exploited as a raw material in the production of low energy belite cements. The clinkers produced were characterised by SEM/EDS and Rietveld QXRD. Water demand, initial setting time, soundness and compressive strength were measured on both cement and cement paste. The hydration behaviour of these cements as well as their leaching potential is addressed in a separate work.

2. Materials and methods

The raw materials used in the preparation of the raw meals were limestone, flysch and EAFS. The chemical analysis was performed by X-ray fluorescence spectrometry (XRF, Philips PW 2400). The crystalline phases of the raw materials were identified by X-ray diffraction analysis (D5000 Siemens). Qualitative analysis was performed by the DIFFRACplus EVA® software (Bruker-AXS) based on the ICDD Powder Diffraction File. The mineral phases were quantified using a Rietveld-based quantification routine with the TOPAS® software (Bruker-AXS). This routine is based on the calculation of a single mineral-phase pattern and the refinement of the pattern using a non-linear least squares routine [24]. A number of corrections, including adjustments to the instrument's geometry, background, sample displacement, detector type and mass absorption coefficients of the refined phases, were applied in order to achieve the optimum pattern fitting. Diffraction patterns were measured in 2θ range of 5–70° using CuKα radiation of 40 kV and 30 mA, with a 0.01° step size and step time of 1 deg/min.

The design of the raw meals was based on the predictions of Bogue equations. In order to produce high belite cement, the lime saturation factor (LSF) was adjusted between 78% and 83% [7] whereas the alumina (AR) and silica ratios (SR) varied from 1.00% to 1.87% and 1.96% to 3.29%, respectively, similar to those adopted in the production of OPC. The quality indices LSF, AR and SR were calculated according to Eqs. (1)–(3) [5,23]:

$$\mathrm{LSF} = \frac{\%\mathrm{CaO}}{2.8 * \%\mathrm{SiO_2} + 1.2 * \%\mathrm{Al_2O_3} + 0.65 * \%\mathrm{Fe_2O_3}} \quad (1)$$

$$\mathrm{SR} = \frac{\%\mathrm{SiO_2}}{\%\mathrm{Al_2O_3}+\%\mathrm{Fe_2O_3}} \quad (2)$$

$$\mathrm{AR} = \frac{\%\mathrm{Al_2O_3}}{\%\mathrm{Fe_2O_3}} \quad (3)$$

Based on the above and on the chemical analysis of the raw materials, an MS Excel© worksheet was used in order to derive the syntheses of the raw meals. Three types of clinker were prepared: one as a reference (named BC), a second with the addition of 5 wt.% EALS (BC5) and third with the addition of 10 wt.% EAFS (BC10). The obtained meal contents in limestone/flysch/EAFS were in wt.%: 84.0/16.0/0.0, 80.5/14.5/5.0 and 77.0/13.0/10.0 for BC, BC5 and BC10, respectively. The results of the quality indices are presented in Table 3. BC10 presents a maximum in terms of EAFS addition (10 wt.%), while keeping LSF within the desired limits. The mineralogical phases of the clinkers were calculated also by the Rietveld method, besides the estimations derived from the Bogue equations (Table 4).

For the preparation of the clinkers, raw materials were individually milled in a Siebtechnik® planetary mill at a particle size below 90 μm. After mixing and homogenizing, pellets of approximately 15–20 mm diameter were formed by hand with a minimum water addition. The pellets were dried for 24 h at 110 °C, followed by calcination at 1000 °C for 4 h. Firing of the clinker was performed in a Nabertherm® type Super Kanthal resistance furnace at 1380 °C. Optimum clinkering temperature was determined by burnability tests at 1280 °C, 1300 °C, 1320 °C, 1350 °C, 1380 °C and 1400 °C, with 40 min of soaking time to determine the free lime content according to ASTM C114-03, as well as by SEM observations which evaluated the quality of the clinker. For the stabilization of α′- and β- C_2S polymorphic forms, fast cooling was applied by simultaneously applying blown air and crushing by means of a hammer.

Clinkers were characterised by QXRD and SEM/EDS microanalysis (Jeol JSM 6300 and LINK PentaFET 6699, Oxford Instruments). Carbon coated samples, fractured, polished as well as etched with 1% Nital, were used. All EDS analyses were undertaken well away from phase boundaries. In the case of belite and alite crystals, spot analyses were performed. In the case of the interstitial phase, due to the micro-crystalline texture of the individual phases finely distributed within the amorphous one, analysis of an approximately 4 μm × 4 μm area away from alite and belite boundaries was performed. The default standards of LINK ISIS have been used.

For the preparation of the cement, clinker was milled by means of the aforementioned planetary mill to finesse in the range of 4000–4100 cm^2/g. After milling, 5 wt.% gypsum with grain size lower than 90 μm was added. Specific surface (Blaine method) was measured according to EN 196-6 [25], setting time and soundness according to EN 196-3 [26] and compressive strength according to EN 196-1 [27].

Table 1
Chemical composition of the raw materials (wt.%).

Oxides	EAFS	Limestone	Flysch
CaO	32.50	48.90	5.55
FeO_{total}	26.30	1.00	5.90
SiO_2	18.10	9.00	58.25
Al_2O_3	13.30	1.36	13.75
MnO	3.94	n.d.	n.d.
MgO	2.53	0.65	2.86
Cr_2O_3	1.38	n.d.	n.d.
P_2O_5	0.48	n.d.	n.d.
TiO_2	0.47	n.d.	n.d.
SO_3	0.44	n.d.	0.05
Cl	0.14	n.d.	n.d.
BaO	0.14	n.d.	n.d.
Na_2O	0.13	0.10	1.10
K_2O	n.d.	0.15	2.50
V_2O_5	0.06	n.d.	n.d.
LOI	0.00	38.00	9.80
Total	99.91	99.16	99.76

LOI, loss on ignitions; n.d., not determined.

3. Results and discussion

3.1. Characterisation of raw materials

XRF chemical analyses of the raw materials, limestone, flysch and EAFS are given in Table 1. It is observed that EAFS contains elements such as Cr, P, Ti, S and Ba that are considered as dopants for belite activation. The introduction of such ions into the crystal lattice of C_2S, can stabilise α′- and β- polymorphs; α′-C_2S being more active than β-C_2S [7,28]. XRD analyses of the raw materials are shown in Fig. 1 whereas the results for the semi-quantitative mineralogical analysis are presented in Table 2. The main mineralogical phases identified are calcite and quartz for limestone, quartz, illite, dolomite, albite and clinochlore for flysh. EAFS contains significant amounts of larnite (β-belite), gehlenite, wüstite, magnetite, and brownmillerite. The Rietveld analysis results are 41.0 wt.%, 14.7 wt.%, 12 wt.%, 10.0 wt.% and 9.4 wt.% for the above phases, respectively.

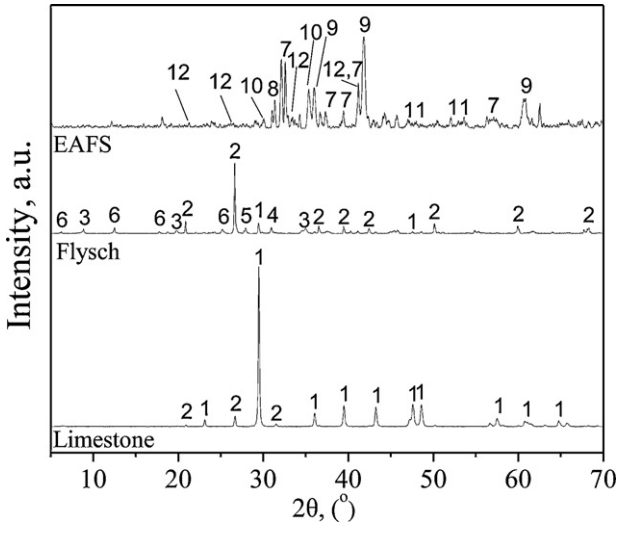

Fig. 1. XRD patterns of the raw materials. The main minerals identified are: 1, calcite ($CaCO_3$); 2, quartz (SiO_2); 3, illite ($(K,H_3O)(Al,Mg,Fe)_2(Si,Al)_4O_{10}((OH)_2,(H_2O))$); 4, dolomite ($CaMg(CO_3)_2$); 5, albite ($NaAlSi_3O_8$); 6, clinochlore ($Mg_{2.5}Fe_{1.65}Al_{1.5}Si_{2.2}Al_{1.8}O_{10}(OH)_8$); 7, larnite (β-$Ca_2SiO_4$); 8, gehlenite ($Ca_2Al(AlSi)O_7$); 9, wüstite (FeO); 10, magnetite (Fe_3O_4); 11, brownmillerite ($Ca_2(AlFe_3)_2O_5$); 12, mayenite ($Ca_{12}Al_{14}O_{33}$).

Table 2
Mineralogical composition of the raw materials, wt.%, according to Rietveld analysis, normalised.

Limestone		Flysch		EAFS	
Calcite	90.5	Illite	34.1	Larnite	41.0
Quartz	5.7	Quartz	28.2	Gehlenite	14.7
Illite	1.1	Kaolinite	8.5	Wüstite	12.0
Microcline	1.1	Dolomite	6.8	Magnetite	10.0
Muscovite	0.6	Albite	6.7	Brownmillerite	9.4
Kaolinite	0.5	Calcite	5.9	Mayenite	7.2
Hematite	0.2	Microcline	5.7	Merwinite	3.7
Clinochlore	0.2	Muscovite	2.2	Spinel	2.0
Cristobalite	0.1	Clinochlore	1.3		
		Hematite	0.6		
Total	100		100		100

3.2. Clinker quality as a function of firing temperature

The composition of the produced clinkers, as well as the quality indices are presented in Table 3. In the firing tests, the maximum free lime content was 1.6 wt.% for both BC and BC10 at 1280 °C. For the temperature range 1300–1400 °C, free lime varied from 0.4 wt.% to 0.2 wt.% for all mixtures tested. For firing higher than 1300 °C, therefore, free lime values are well below the commonly defined threshold of 1 wt.% for OPC clinker.

In Figs. 2 and 3, backscattered electron images revealing the development of clinker microstructure at different firing temperatures for BC and BC10 are presented. In both cases for temperatures up to 1320 °C, clinker microstructure is poorly developed. An extended interstitial phase is also observed. At temperatures exceeding 1350 °C, the dissolution and transport phenomena through the melt are enhanced: the precipitation of stable, rounded belite is apparent in conjunction with the formation, at a lesser extent, of angular alite. The resulting microstructures are characterised by uniform distribution and development of the phases. Firing at 1400 °C has no detectable difference in terms of phase morphology and growth compared to 1380 °C. Comparing BC and BC10 microstructures, slag addition disfavours alite formation and promotes the formation of the interstitial phase as well as that of

Table 3
Composition of raw metals, resulted chemical composition of the produced clinkers and quality indexes results.

	0 wt.% BC	5 wt.% BC5	10 wt.% BC10
Raw material			
EAFS	0.0	5.0	10.0
Limestone	84.0	80.5	77.0
Flysch	16.0	14.5	13.0
Oxides			
SiO_2	25.38	24.41	23.48
Al_2O_3	5.03	5.52	6.00
Fe_2O_3	2.68	4.38	6.00
CaO	63.09	61.47	59.92
MgO	1.51	1.57	1.62
K_2O	0.79	0.71	0.63
Na_2O	0.39	0.36	0.34
SO_3	0.01	0.04	0.07
MnO	0.00	0.29	0.57
Cr_2O_3	0.00	0.10	0.20
P_2O_5	0.00	0.04	0.07
TiO_2	0.00	0.03	0.07
Cl	0.00	0.01	0.02
BaO	0.00	0.01	0.02
V_2O_5	0.00	0.00	0.01
Total	98.88	98.95	99.01
Quality indexes			
LSF	80.13	79.00	78.10
AR	1.87	1.26	1.00
SR	3.29	2.47	1.96

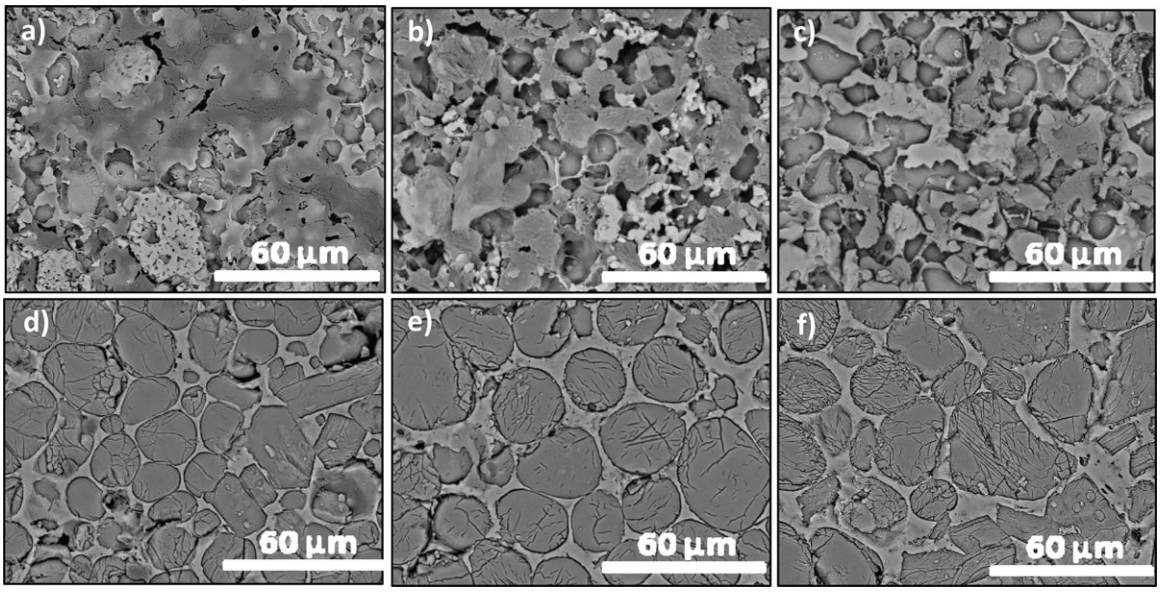

Fig. 2. Backscattered images of preliminary firings. BC clinker formed at different firing temperatures: (a) 1280 °C, (b) 1300 °C, (c) 1320 °C, (d) 1350 °C, (e) 1380 °C and (f) 1400 °C.

belite. The size of crystals varies from 5 μm to 50 μm. These values are typical for a good quality clinker. According to the above results, it was decided that the firing of the clinker should be performed at 1380 °C.

3.3. Clinker characterisation

The XRD patterns of the prepared clinkers are depicted in Fig. 4. Table 4 presents the mineralogical compositions calculated by Rietveld and the estimations obtained by Bogue equations. As expected, discrepancies exist between the results obtained by Bogue and Rietveld, the most significant being Bogue's underestimation of C_3S and overestimation of C_2S. These are attributed to the fact that Bogue's method is based on ideal stoichiometries for the clinker phases, without taking into consideration solid solutions, and also implies a certain reaction and solidification path. On the other hand, Rietveld analysis can reflect the changing conditions induced by the different raw materials as well as the non-equilibrium conditions during firing and cooling. Nonetheless, the qualitative trend is soundly predicted by Bogue.

Based on the X-ray diffraction results, the main mineralogical phases identified were: alite (C_3S), belite (C_2S), tricalcium aluminate (C_3A), and tetracalcium-alumino-ferrite (C_4AF). The specific polymorphism is important as affects the hydration and, as a consequence, the development of microstructure and mechanical properties. The main polymorphic form of stabilised alite is tri-

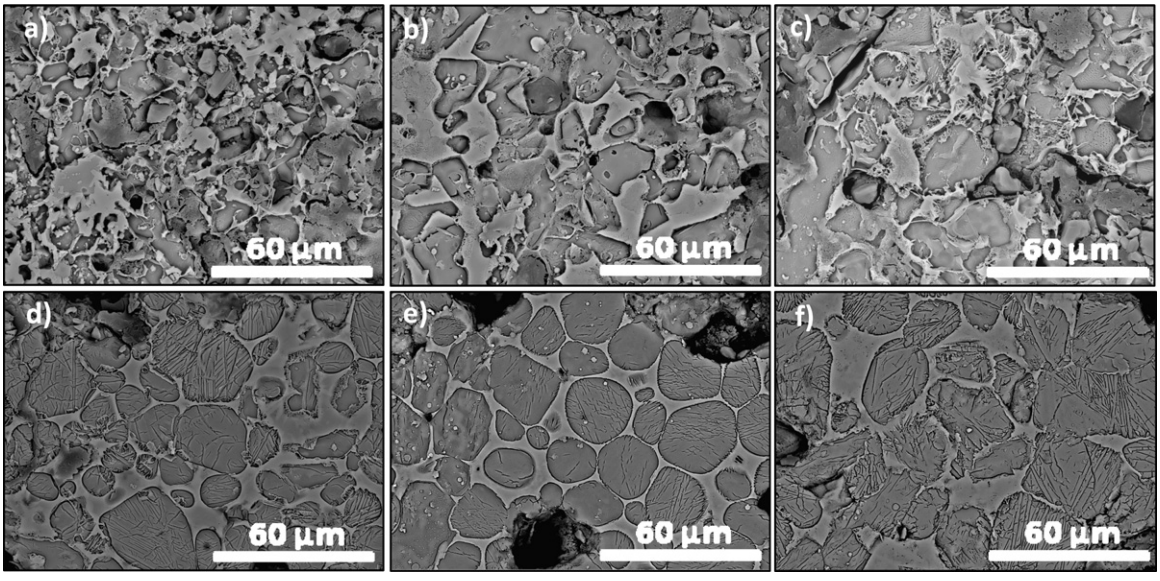

Fig. 3. Backscattered images of preliminary firings. BC10 clinker formed at different firing temperatures: (a) 1280 °C, (b) 1300 °C, (c) 1320 °C, (d) 1350 °C, (e) 1380 °C and (f) 1400 °C.

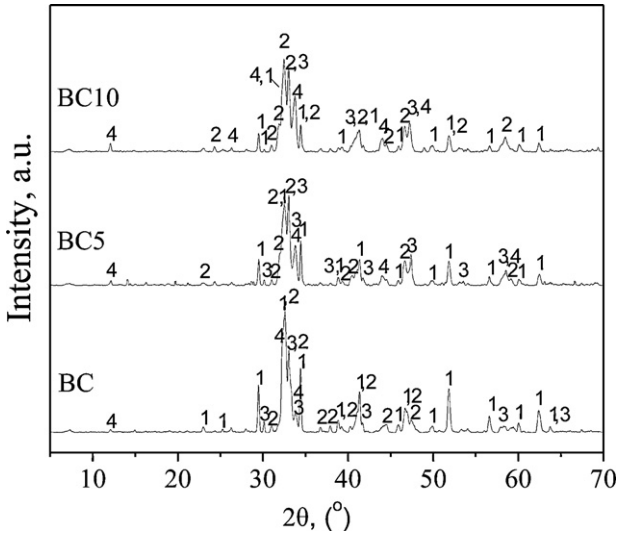

Fig. 4. X-ray patterns of the prepared clinkers. The main minerals identified: 1, C_3S; 2, C_2S; 3, C_3A; 4, C_4AF.

clinic (T), which decreases as the slag content increases towards the monoclinic (M) one. This is expected to affect early strength development towards lower values [29]. The rhombohedral (R) alite is reacting slightly more rapidly compared with T and M polymorphic forms [29,30] but without a significant effect in the present case due to the low content. Regarding belite, mainly the α′ polymorph was identified. The γ- and β-C_2S polymorphs were also detected and increased as the slag content rose. Beta, β- and α′-C_2S play an important role during late days of hydration. On the contrary, γ-C_2S does not present notable hydraulic properties. C_3A was formed as cubic and orthorhombic in BC, whereas only the orthorhombic form was found in BC5 and BC10. The predominance of orthorhombic C_3A in the last two mentioned clinkers was most probably due to the higher sulphate content in the EAFS which inhibits the formation of cubic C_3A [31]. The identified orthorhombic C_3A polymorph will react faster in the presence of gypsum than its cubic counterpart [32]. In general, the increase in EAFS content results in a decrease in C_3S and C_3A and an increase in C_4AF; this is attributed to the high iron content of the slag.

Table 4
Estimated (Bogue) and calculated (Rietveld) mineralogical composition of the prepared clinkers.

Phases	BC		BC5		BC10	
	Rietveld	Bogue	Rietveld	Bogue	Rietveld	Bogue
C_3S (M1)	1.0		3.4		4.0	
C_3S (M3)	0.3		1.3		1.5	
C_3S-T	33.3		20.8		15.4	
C_3S-R	0.7		3.4		0.9	
Total	35.30	27.43	28.90	22.39	21.80	17.59
C_2S-α'	45.5		41.6		42.2	
C_2S-β	1.9		4.0		5.8	
C_2S-γ	0.0		1.5		0.8	
Total	47.40	54.96	47.10	56.16	48.80	57.32
C_3A – Cubic	2.7		0.0		0.0	
C_3A – Orth.	6.0		4.9		4.3	
Total	8.70	9.13	4.90	7.54	4.30	6.01
C_4AF	7.50	8.49	18.50	13.90	24.10	19.08
Lime	0.4	0.0	0.0	0.0	0.0	0.0
MgO	0.7	0.0	0.6	0.0	1.0	0.0
Total	100	100	100	100	100	100

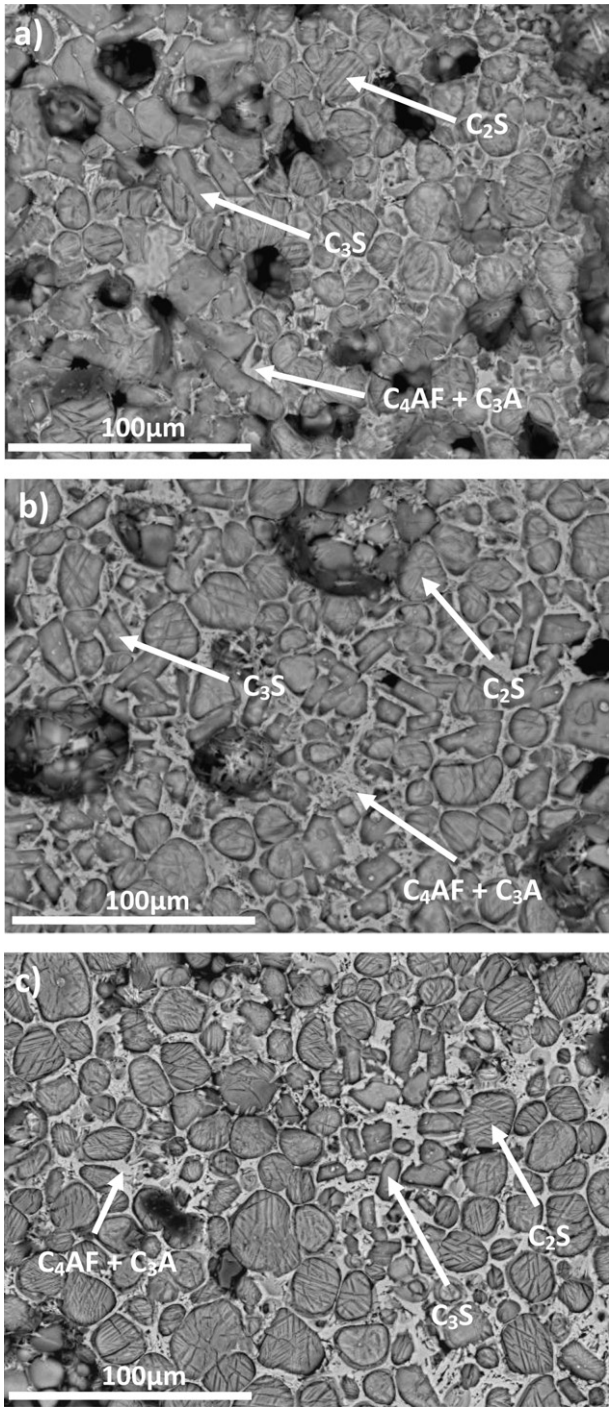

Fig. 5. Backscattered images of clinkers in polished section: (a) BC, (b) BC5 and (c) BC10.

Backscattered electron images (BEI) are presented in Fig. 5a, b and c for BC, BC5 and BC10, respectively. In all cases the microstructures consist predominantly of well-developed crystals of type I belite according to Insley's classification [33]. Their diameter varies from 5 μm to 50 μm. Most of the belite crystals display complex twin lamellae. The formed striations arise as a consequence of phase transformation during cooling. In type I belite, it has been reported that this is a skeleton structure rather than polysynthetic twinning, consisting of beta and alpha forms of belite [33]. Crystals with parallel striations are less noticeable. Angular, euhedral and subhedral alite crystals are also present. In the case of BC10, alite crystals

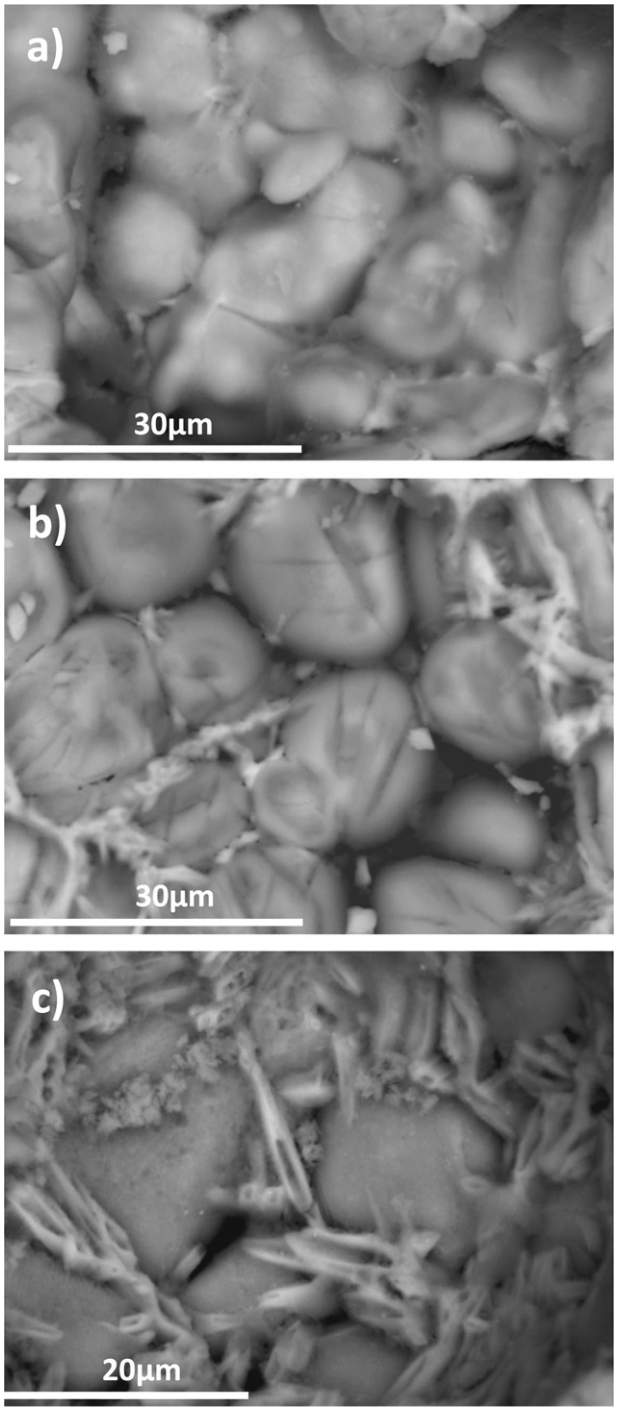

Fig. 6. Backscattered images of clinkers in fractured surface: (a) BC, (b) BC5 and (c) BC10.

contain inclusions of belite in some cases. The crystallised-during-cooling interstitial phase presents a micro-crystalline texture and mainly consists of a mixture of ferrite and C_3A. It partially separates the primary alite and belite crystals. The addition of slag favours the formation of belite and ferrite phases as it disfavours the formation of alite. Ferrite crystals pipework exposed on a broken surface are presented in Fig. 6b and c for BC5 and BC10, respectively. Voids in their structure are presumably occupied by aluminate. The lamellar belite structure is slightly visible. In Fig 6b micro-cracks that developed on the belite crystals are clearly visible. Plausible hypotheses for the formation of these micro-cracks are: (a) as dicalcium silicate crystals are considered to be complex, containing point defects, they undergo inversions on cooling which cause twinning resulting in strain accumulations [34] and (b) they were caused by the etching [33].

Representative EDS micro-analyses of C_3S and C_2S crystals and interstitial phase for each clinker prepared are presented in Table 5. Ferrite and aluminate phases are not presented individually due to the difficulties imposed by their micro-crystalline texture, but analysis of the interstitial phase is denoted as $C_3A + C_4AF$ in the table. As a general remark, it was observed that alite and belite become enriched with iron as the slag content rises, whereas Ba, Cr, Ti and P are more likely to be found in the belite crystals. According to the present QXRD and SEM/EDS results and under the adopted experimental conditions, no clear conclusions can be drawn concerning the influence of slag addition on the belite crystals, although it is a host of elements such as P, S, Cr which are known as belite stabilisers. However, this will be the subject of a forthcoming communication dealing with the composition and substitutions in the individual phases.

3.4. Specific surface, setting time and soundness measurements

In Table 6 the results of water demand, initial setting time and soundness of the cement pastes are presented. To prepare the cement paste with the standard consistency [26] the water demand was 27.6 wt.% for all cases. Initial setting times obtained for BC, BC5 and BC10 were 240 min, 170 min and 20 min, respectively according to EN 197-1 standard in the first 2 cases.

It is observed that the use of slag decreases the setting time, with the BC10 behaving as fast-setting cement. This is attributed to the increase of the molten phase, forming upon cooling higher amounts of C_4AF, and the interaction with C_3A and gypsum during hydration.

In more detail, as early hydration of cement is principally controlled by the amount and activity of C_3A, setting is balanced by the amount and type of sulphate interground with the cement. Tetracalcium-alumino-ferrite (C_4AF) reacts much like C_3A, i.e., forming ettringite in the presence of gypsum. The higher amounts of C_4AF in the clinkers with slag (more than two-fold and three-fold increase for BC5 and BC10, respectively compared to BC) consume also higher amounts of gypsum. Hence, it is likely that setting occurs due to the uncontrolled reaction of the C_3A, after depletion of the sulphate by reaction with the C_4AF. Addition of higher amounts of gypsum or of retarders, possibly of organic nature, could control the setting behaviour.

Expansion was 1 mm for all prepared cements. In order to obtain Blaine of 4000 cm^2/g, 4080 cm^2/g and 4057 cm^2/g, the required milling times were 60 sec, 80 sec and 103 sec for BC, BC5 and BC10, respectively. Notably, increasing the slag addition results in an increased milling time for comparable finesse.

3.5. Compressive strength of the BC, BC5 and BC10 cements

In Fig. 7 the compressive strength results are presented. As expected for belite cements, the early days strength development is significantly lower than that of the OPC. For BC, the results for 2 days were 6.5 MPa whereas for BC5 and BC10 they were even lower, at 2.5 MPa and 1.6 MPa, respectively. However the 28-day results for BC, BC5 and BC10 were 47.5 MPa, 46.6 MPa and 42.8 MPa, respectively, which are comparable to OPC CEMI 32.5N (32.5–52.5 MPa) according to EN 197-1 [35]. These results concur with previously reported results [36–39]. The low early strength development observed in the cements with slag addition is attributed, as in cases of fast setting behaviour, to the extended formation of ferrite. The higher results for BC at early days are attributed to the higher C_3S and C_3A content, compared to BC5 and BC10. Compared to other belite cements incorporating wastes, belite cement with EAFS has

Table 5
Typical EDS micro-analyses for clinkers: (a) BC, (b) BC5 and (c) BC10, in wt.%.

Phase	BC			BC5			BC10		
	C_3S	C_2S	C_4AF+C_3A	C_3S	C_2S	C_4AF+C_3A	C_3S	C_2S	C_4AF+C_3A
NaO	0.10	0.20	0.67	0.11	0.01	0.28	0.09	0.12	0.19
MgO	0.40	0.36	1.45	0.30	0.36	1.53	0.81	0.97	1.35
Al_2O_3	1.23	1.73	20.74	1.66	0.84	20.04	2.25	2.82	18.99
SiO_2	24.05	30.65	5.35	23.66	30.88	4.16	22.49	30.25	4.78
P_2O_5	0.00	0.00	0.00	0.00	0.23	0.00	0.01	0.43	0.00
SO_3	0.00	0.20	0.08	0.00	0.03	0.14	0.10	0.00	0.13
K_2O	1.43	1.44	0.50	1.36	1.35	0.50	1.50	0.81	0.54
CaO	71.25	64.10	59.14	69.97	61.38	56.41	68.01	59.03	53.59
TiO_2	0.00	0.00	0.00	0.04	0.10	0.06	0.08	0.04	0.09
MnO	0.00	0.00	0.00	0.36	0.39	1.35	0.94	0.38	1.38
FeO_{total}	1.54	1.32	12.07	2.19	3.22	15.43	3.34	4.52	18.86
V_2O_5	0.00	0.00	0.00	0.00	0.00	0.00	0.00	0.00	0.02
BaO	0.00	0.00	0.00	0.00	0.09	0.05	0.03	0.13	0.06
Cr_2O_3	0.00	0.00	0.00	0.35	0.22	0.05	0.35	0.50	0.02
Total	100	100	100	100	100	100	100	100	100

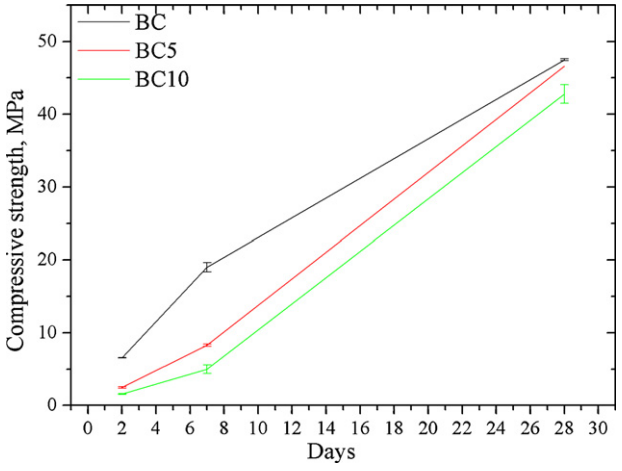

Fig. 7. Compressive strength results of the BC, BC5 and BC10 cements.

Table 6
Physical properties of the cement and cement pastes.

Cement types	BC	BC5	BC10
Specific surface (cm^2/g)	4000	4080	4057
Initial setting time (min)	240	170	20
Water demand (wt.%)	27.6	27.6	27.6
Soundness (mm)	1	1	1

lower early and late compressive strength than belite with Bayer's process red mud [38] (5.0 MPa at 1 day and 53.7 MPa at 28 days) and higher early and late compressive strength than belite cement with boron waste [39] (1.5 MPa at 1 day and 32.3 MPa at 28 days).

4. Conclusion

The production of belite cements with EAFS is feasible and can offer significant environmental advantages. Specifically the characteristics of the cements are as follows:

- Clinkers predominantly contain well-formed belite crystals. Alite crystals are also present.
- The interstitial phase is a mixture of C_4AF and C_3A, and partially separates the primary alite and belite crystals.
- Slag addition favours the formation of the belite and ferrite phase and disfavours the formation of alite, in accordance with Bogue's predictions under the requirement of comparable quality indices.
- Early days compressive strength results are low, as is expected for belite cements, however the 28-day results for BC, BC5 and BC10 were 47.5 MPa, 46.6 MPa and 42.8 MPa, respectively which are comparable to EN 197-1, OPC CEMI 32.5N ones.
- The addition of slag did not affect the water demand of the cements and soundness did not exceed 1 mm, although setting time was decreased for BC10, which behaved like "flash set" cement.
- The fast setting that occurred for the cements with slag addition is attributed to the extended formation of the molten phase which forms ferrite upon cooling and the interaction with C_3A and gypsum during hydration.

Acknowledgements

R.I. Iacobescu and R. Saban acknowledge the support of the Sectoral Operational Programme for Human Resources Development 2007–2013 of the Romanian Ministry of Labour, Family and Social Protection through the Financial Agreement POSDRU/6/1.5/S/16. D. Koumpouri and G.N. Angelopoulos acknowledge the support of University of Patras through the "Karatheodoris" 2011 research program. Y. Pontikes is thankful to the Research Foundation – Flanders for the post-doctoral fellowship. TITAN Cement Company S.A. and SOVEL S.A. metallurgy industries are gratefully acknowledged for providing raw materials as well as their technical assistance.

References

[1] International Cement Review, The Global Cement Report, ninth ed., World Overview, 2011.
[2] J.S. Damtoft, J. Lukasik, D. Herfort, D. Sorrentino, E.M. Gartner, Sustainable development and climate change initiatives, Cem. Concr. Res. 38 (2008) 115–127.
[3] V.M. Malhotra, Global warming, and role of supplementary cementing materials and superplasticisers in reducing greenhouse gas emissions from the manufacturing of portland cement, Int. J. Struct. Eng. 1 (2010) 116–130.
[4] M. Schneider, M. Romer, M. Tschudin, H. Bolio, Sustainable cement production—present and future, Cem. Concr. Res. 41 (2011) 642–650.
[5] J.I. Bhatty, F.M. Miller, S.H. Kosmatka, Innovations in Portland Cement Manufacturing, Portland Cement Association, 2004.
[6] C.D. Popescu, M. Muntean, J.H. Sharp, Industrial trial production of low energy belite cement, Cem. Concr. Compos. 25 (2003) 689–693.
[7] C.D. Lawrence, The production of low-energy cements, in: Lea's Chemistry of Cement and Concrete, 4th ed., Butterworth-Heinemann, Oxford, 2003.
[8] H. Uchikawa, Management strategy in cement technology for the next century. Part 3, World Cem. November (1994) 47.
[9] E. Gartner, Industrially interesting approaches to "low-CO_2" cements, Cem. Concr. Res. 34 (2004) 1489–1498.
[10] K. Quillin, Performance of belite-sulfoaluminate cements, Cem. Concr. Res. 31 (2001) 1341–1349.
[11] US Environmental Protection Agency, Materials characterization paper, in support of the final rulemaking: identification of nonhazardous secondary

materials that are solid waste steel furnace Slag (used as an ingredient in clinker manufacture and bituminous concrete), in: Steel Furnace Slag, 2011, pp. 1–5.
[12] I. Akln Altun, Y. Ismail, Study on steel furnace slags with high MgO as additive in Portland cement, Cem. Concr. Res. 32 (2002) 1247–1249.
[13] H. Motz, J. Geiseler, Products of steel slags an opportunity to save natural resources, Waste Manag. 21 (2001) 285–293.
[14] European Slag Association, www.euroslag.org, 2011.
[15] International Iron and Steel Institute, IISI Steel statistical Yearbook, Brussels, Belgium, 2004. http://www.worldsteel.org/.
[16] Hellenic Cement Industry Association, http://www.hcia.gr.
[17] S.R. Rao, Waste management series 7, in: Resource Recovery and Recycling from Metallurgical Wastes, 2006.
[18] J. Paceagiu, E. Radulescu, A.M. Dragomir, R. Hotnog, Implications of the use of steel slags to clinker manufacture: laboratory test results, Romanian J. Mater. 40 (2010) 306–314.
[19] C. Shi, Corrosion resistant cement made with steel mill by-products, Proceedings of International Symposium of the Utilisation of Metallurgical Slags, Chinese Society for Metals, Beijing, 1999, pp. 171–178.
[20] D. Adolfsson, N. Menad, E. Viggh, B. Björkman, Steelmaking slags as raw material for sulphoaluminate belite cement, Adv. Cem. Res. 19 (2007) 147–156.
[21] European Parliament, Directive 2003/53/EC of the European Parliament and of the Council, 2003.
[22] U.S. Department of Health and Human Services, Centers for Disease Control and Prevention, National Institute for Occupational Safety and Health, NIOSH, Criteria document update, Occupational Exposure to Hexavalent Chromium, External Review Draft, 2008.
[23] B.W. Nicholas, Understanding Cement, WHD Microanalysis Consultant Ltd., United Kingdom, 2010.
[24] C.R. Ward, J.C. Taylor, C.E. Matulis, L.S. Dale, Quantification of mineral matter in the Argonne Premium Coals using interactive Rietveld-based X-ray diffraction, Int. J. Coal Geol. 46 (2001) 67–82.
[25] European Committee for Standardization, EN 196-6, Methods of testing cement. Determination of Fineness, 1989.
[26] European Committee for Standardization, EN 196-3, Methods of testing cement. Part 3. Determination of Setting Time and Soundness, 1994.
[27] European Committee for Standardization, EN 196-1, Methods of testing cement. Part 1. Determination of Strength, 1994.
[28] S.N. Ghosh, P.B. Rao, A.K. Paul, K. Raina, Review. The chemistry of dicalcium silicate mineral, J. Mater. Sci. 14 (1979) 1554–1566.
[29] T. Stanek, P. Sulovský, The influence of the alite polymorphism on the strength of the Portland cement, Cem. Concr. Res. 32 (2002) 1169–1175.
[30] R.T.H. Aldous, The hydraulic behaviour of rhombohedral alite, Cem. Concr. Res. 13 (1983) 89–96.
[31] L. Gobbo, L. Sant' Agostino, L. Garcez, C_3A polymorphs related to industrial clinker alkalies content, Cem. Concr. Res. 34 (2004) 657–664.
[32] A. Kirchheim, V. Fernàndez-Altable, P. Monteiro, D. Dal Molin, I. Casanova, Analysis of cubic and orthorhombic C_3A hydration in presence of gypsum and lime, J. Mater. Sci. 44 (2009) 2038–2045.
[33] D.H. Campbell, Microscopical Examination and Interpretation of Portland Cement and Clinker, Portland Cement Association, Skokie, IL 60077-1083, USA, 1999.
[34] S.N. Ghosh, Advances in Cement Technology: Critical Reviews and Case Studies on Manufacturing, Quality Control, Optimisation and Use, New Delhi, India, 1983.
[35] European Committee for Standardization, EN 197-1, Cement. Part 1. Composition, Specifications and Conformity Criteria for Common Cements, 2000.
[36] J. Stark, A. Müller, R. Schrader, K.R. Rumpler, Existence Conditions of Hydraulically Active Belite, Zement-Kalk-Gips, Bauverlag GmbH, Wiesebaden, Germany, 1981.
[37] I. Vangelatos, Valorisation of Red Rud in the Cement Industry, Department of Chemical Engineering, University of Patras, Patras, 2008.
[38] I. Vangelatos, Y. Pontikes, G.N. Angelopoulos, Ferroalumina as a raw material for the production of "Green" belite type cements, in: SERES' 09. I. International Ceramic, Glass, Porcelain Enamel, Glaze and Pigment Congress, Eskisehir, Turkey, 2009.
[39] T. Kavas, I. Vangelatos, S. Koyas, Y. Tabak, G.N. Angelopoulos, Wastes from alumina and boron production as raw materials for belite cement, in: J. Heinrich, C. Aneziris (Eds.), 10th Conference and Exhibition of the European Ceramic Society, Berlin, Germany, 2007, pp. 1799–1803.